FLEXIBLE ELECTRONICS

Chip-less wireless electronic skins by remote epitaxial freestanding compound semiconductors

Yeongin Kim[1,2,3]†, Jun Min Suh[1,2]†, Jiho Shin[1,2]†, Yunpeng Liu[1,2]†, Hanwool Yeon[1,2,4], Kuan Qiao[1,2], Hyun S. Kum[1,2,5], Chansoo Kim[1,2], Han Eol Lee[1,2,6], Chanyeol Choi[7], Hyunseok Kim[1,2], Doyoon Lee[1,2], Jaeyong Lee[1], Ji-Hoon Kang[2], Bo-In Park[2], Sungsu Kang[8], Jihoon Kim[8], Sungkyu Kim[9], Joshua A. Perozek[7], Kejia Wang[1,10], Yongmo Park[1], Kumar Kishen[1], Lingping Kong[1], Tomás Palacios[7], Jungwon Park[8,11], Min-Chul Park[12], Hyung-jun Kim[12,13], Yun Seog Lee[14], Kyusang Lee[15], Sang-Hoon Bae[1,16], Wei Kong[1,17], Jiyeon Han[18]*, Jeehwan Kim[1,2,19]*

Recent advances in flexible and stretchable electronics have led to a surge of electronic skin (e-skin)–based health monitoring platforms. Conventional wireless e-skins rely on rigid integrated circuit chips that compromise the overall flexibility and consume considerable power. Chip-less wireless e-skins based on inductor-capacitor resonators are limited to mechanical sensors with low sensitivities. We report a chip-less wireless e-skin based on surface acoustic wave sensors made of freestanding ultrathin single-crystalline piezoelectric gallium nitride membranes. Surface acoustic wave–based e-skin offers highly sensitive, low-power, and long-term sensing of strain, ultraviolet light, and ion concentrations in sweat. We demonstrate weeklong monitoring of pulse. These results present routes to inexpensive and versatile low-power, high-sensitivity platforms for wireless health monitoring devices.

Electronic skin (e-skin)–based health monitoring platforms have recently emerged, including flexible and stretchable sensors (*1*), electronic circuits (*2*), and skin-compatible adhesive patches (*3*, *4*) that laminate conformally onto the skin. Their applications include biophysical tracking of fitness and wellness (*5*), as well as clinical management (*4*, *6*). A key technical requirement for the broader use of e-skins in our daily lives is the capability to communicate data wirelessly. A major issue in conventional wireless e-skins is that they require rigid integrated circuit chips—near-field communication (NFC) or radio frequency identification (RFID) chips, microprocessors, or analog-to-digital converters (ADCs), for example—which can compromise overall flexibility. Moreover, given the power constraint in wireless e-skin systems, the high power consumption by these chips, which contain thousands of transistors (*7*), often leads to reduced sensitivity (due to the power–sensitivity trade-off in ADCs) (*8*), substantial heat generation (*9*), and reduced communication distance (*10*). To address these issues, inductor-capacitor (LC) resonator–based chip-less wireless e-skin sensors have been studied (*11*), but demonstrated applications are restricted to strain and pressure sensing with relatively low sensitivity owing to the limitations of capacitive sensor designs.

We report a chip-less wireless e-skin technology based on surface acoustic wave (SAW) sensors that achieves marked improvement in strain sensitivity, power efficiency, versatility as a sensing platform for a broad range of external stimuli, and long-term wearability. This is achieved by integrating a freestanding ultrathin single-crystalline piezoelectric membrane of gallium nitride (GaN) on a flexible patch as the material for passive wireless sensing. The ultrathin GaN epitaxial layers are grown on graphene-coated GaN substrates by remote homoepitaxy and are easily released from the weak graphene–GaN interface by a two-dimensional (2D) material–based layer transfer (2DLT) process (*12*).

Figure 1A and fig. S1 show schematic illustrations comparing conventional chip-based wireless e-skins and our SAW-based chip-less wireless e-skin (see table S1 for additional details). Chip-based wireless e-skins integrate NFC or RFID chips, circuit elements (diodes, resistors, and capacitors), sensors, and radio frequency antenna on silicone patches (*1*). The large size and rigidity of these chips compromise conformal lamination of e-skin on skin and necessitate thick silicone patches (300 to 500 μm), which disturb skin function over time owing to sweat impermeability and occlusion. Moreover, they consume substantial power.

In our SAW-based chip-less wireless e-skin, an ultrathin GaN SAW sensor replaces the chips, circuit components, and sensors. The changes in the resonant frequency of the GaN SAW sensor yield information about mechanical, optical, and biochemical stimuli (see supplementary text in the supplementary materials for the detailed mechanism). The ultrathin and light functional layers (GaN and metal electrodes) can be integrated on a thin patch of polydimethylsiloxane (PDMS; ~20 μm) with perforations that allow removal of sweat and skin by-products (*13*), thereby improving the softness, skin-conformability, and long-term wearability compared with chip-based e-skins, while also consuming considerably less power.

Wireless SAW sensors have traditionally relied on thick, non-freestanding GaN films that are tethered to the wafer, which were difficult to integrate on flexible e-skins. We estimated that the GaN film thickness required for conformal skin adhesion is 300 nm (Fig. 1B; see supplementary materials for detailed calculation). Remote epitaxy can yield single-crystalline GaN membranes with a thickness of <300 nm and reduce material cost for GaN films (*12*).

We successfully performed the remote epitaxy of 200-nm-thick GaN membrane on graphene-coated GaN substrates, followed by exfoliation via 2DLT (fig. S2). High-resolution x-ray diffraction (HRXRD) phi scan data in Fig. 1C shows the perfect single-crystallinity of GaN on graphene. Figure 1D shows cross-sectional transmission electron microscopy (TEM) and associated selective-area diffraction images of the exfoliated GaN membrane on metal support layers indicating solely oriented atomic planes of GaN nanomembrane. Atomic force microscopy analysis (fig. S3) also confirms the atomically flat surface of GaN. These properties are important for high-performance electromechanical and optoelectronic devices. We further verified the capability of our GaN membranes to laminate conformally on skin by attaching them on a skin replica made of Ecoflex silicone [see methods for preparation steps and Fig. 1E for scanning electron microscopy

[1]Department of Mechanical Engineering, Massachusetts Institute of Technology, Cambridge, MA 02139, USA. [2]Research Laboratory of Electronics, Massachusetts Institute of Technology, Cambridge, MA 02139, USA. [3]Department of Electrical Engineering and Computer Science, University of Cincinnati, Cincinnati, OH 45219, USA. [4]School of Materials Science and Engineering, Gwangju Institute of Science and Technology, Gwangju 61005, South Korea. [5]Department of Electrical and Electronic Engineering, Yonsei University, Seoul 03722, South Korea. [6]Division of Advanced Materials Engineering, Jeonbuk National University, Jeonju 54896, South Korea. [7]Department of Electrical Engineering and Computer Science, Massachusetts Institute of Technology, Cambridge, MA 02139, USA. [8]School of Chemical and Biological Engineering, Institute of Chemical Process, Seoul National University, Seoul 08826, South Korea. [9]Department of Nanotechnology and Advanced Materials Engineering, Sejong University, Seoul 05006, South Korea. [10]School of Micro-Nano Electronics, Zhejiang University, Hangzhou 311200 Zhejiang, People's Republic of China. [11]Center for Nanoparticle Research, Institute for Basic Science (IBS), Seoul 08826, South Korea. [12]Post-Silicon Semiconductor Institute, Korea Institute of Science and Technology (KIST), Seoul 02792, South Korea. [13]Division of Nano and Information Technology, KIST School, Korea University of Science and Technology, Seoul 02792, South Korea. [14]Department of Mechanical Engineering, Seoul National University, Seoul 08826, South Korea. [15]Department of Electrical and Computer Engineering, University of Virginia, Charlottesville, VA 22904, USA. [16]Department of Mechanical Engineering and Materials Science, Institute of Materials Science and Engineering, Washington University in St. Louis, MO 63139, USA. [17]Department of Materials Science and Engineering, Westlake University, Hangzhou 310024 Zhejiang, People's Republic of China. [18]Skincare Division, Amorepacific R&D Center, Yongin 17074, South Korea. [19]Department of Materials Science and Engineering, Massachusetts Institute of Technology, Cambridge, MA 02139, USA.
*Corresponding author. Email: jeehwan@mit.edu (Je.K.); sviviria@amorepacific.com (J.H.) †These authors contributed equally to this work.

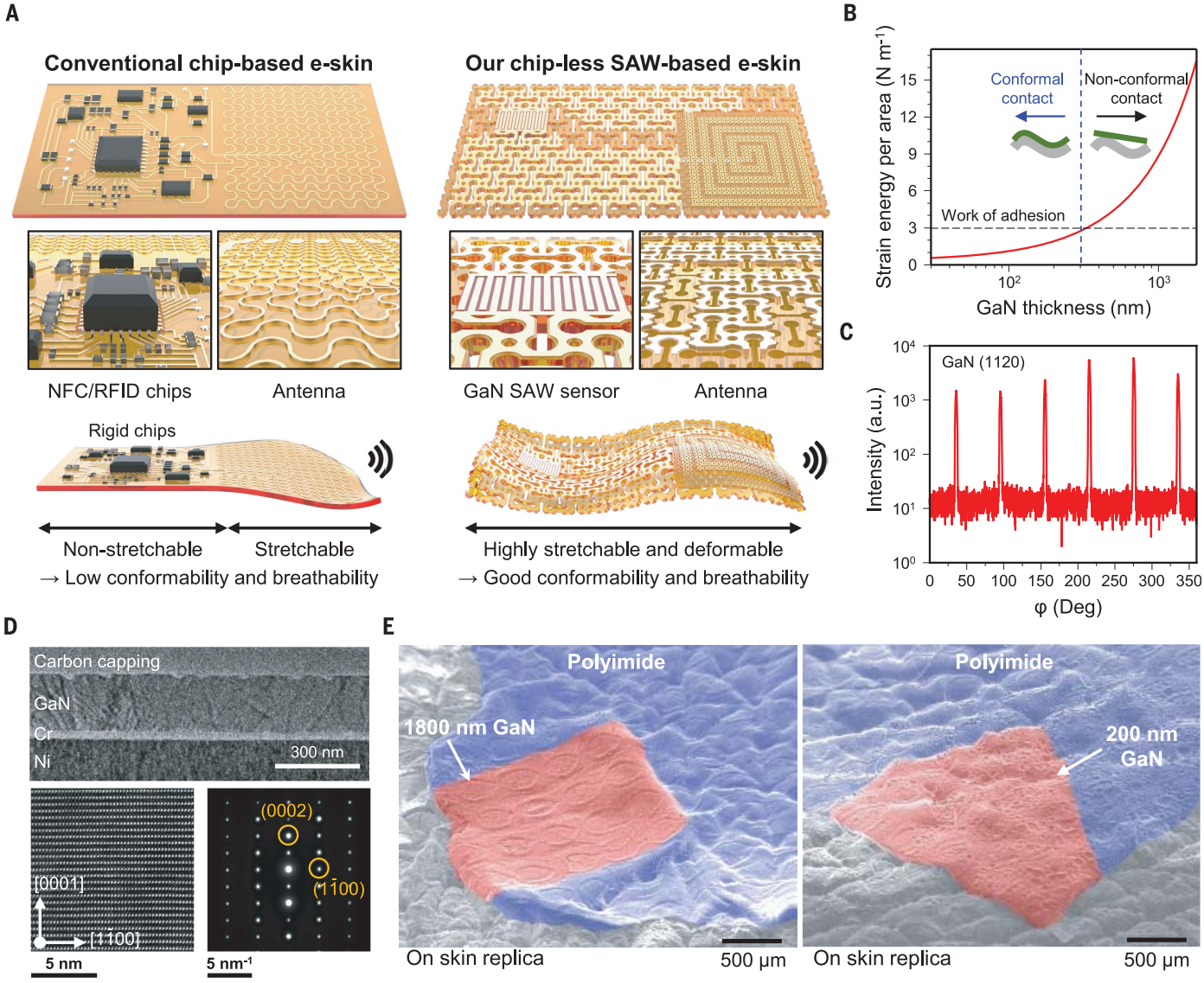

Fig. 1. Chip-less wireless e-skin based on single-crystalline freestanding nanomembranes of GaN and its mechanical properties. (**A**) Comparison between (left) conventional wireless e-skin based on integrated circuit chips and (right) our chip-less wireless e-skin based on surface acoustic wave (SAW) devices made of GaN freestanding membranes. (**B**) Estimation of minimum GaN thickness required for conformal lamination on human skin. Strain energies on curved surfaces per area depending on GaN thickness and the work of adhesion of a PDMS skin patch were calculated and compared. (**C**) HRXRD phi scan of 200-nm-thick remote epitaxial GaN film. a.u., arbitrary units. (**D**) TEM image and associated selective-area diffraction images of the freestanding 200-nm-thick GaN nanomembrane. (**E**) SEM images of GaN e-skins with (left) 1800-nm-thick and (right) 200-nm-thick GaN attached to skin replica samples. The 1800-nm-thick GaN film (left) cannot fully conform to the microscale features of skin, whereas the 200-nm-thick film (right) can deform to follow the pits and curvatures.

(SEM) images]. We integrated our resulting ultrathin GaN membranes into our e-skin (figs. S2 and S4 to S8; see methods for more details).

To study the optoelectronic performance of our GaN nanomembrane device, we fabricated GaN-metal Schottky junction diodes using 200-nm-thick membranes of single-crystalline GaN, obtained by means of remote epitaxy and 2DLT, and polycrystalline GaN, obtained on poor-growth substrates, and compared their ultraviolet (UV) sensitivities. UV radiation is an important health indicator that existing chip-less wireless e-skins based on an LC resonator lack the semiconductor component to detect. Our UV sensing results (Fig. 2A) indicate a UV responsivity of 10.06 A W^{-1} at 15.90 mW/cm^2 for a single-crystalline GaN diode, which is 37-fold higher than that of a polycrystalline GaN diode. This responsivity is also higher than those reported for e-skin sensors based on polycrystalline inorganic materials (*14*) or single-crystalline Si, which has poor optical absorption in the UV wavelength regimes (*15*), and comparable to that of the state-of-the-art single-crystalline GaN UV sensors on "rigid" wafers (*16*). A single-crystalline GaN diode also exhibits higher UV sensing speed, recovery time, and selectivity (for UV light over white light) than those of a polycrystalline GaN diode, as illustrated in Fig. 2, B and C.

The excellent piezoelectricity and perfect single-crystallinity of our ultrathin GaN film enable wireless communication without NFC or RFID chips. We conceived our chip-less wireless e-skin by (i) discovering the formation of highly sensitive SAWs on freestanding ultrathin single-crystalline piezoelectric GaN membranes and (ii) reinventing the freestanding SAW device as a biosensing platform. Upon successful lamination on the human body, our e-skin can generate SAW

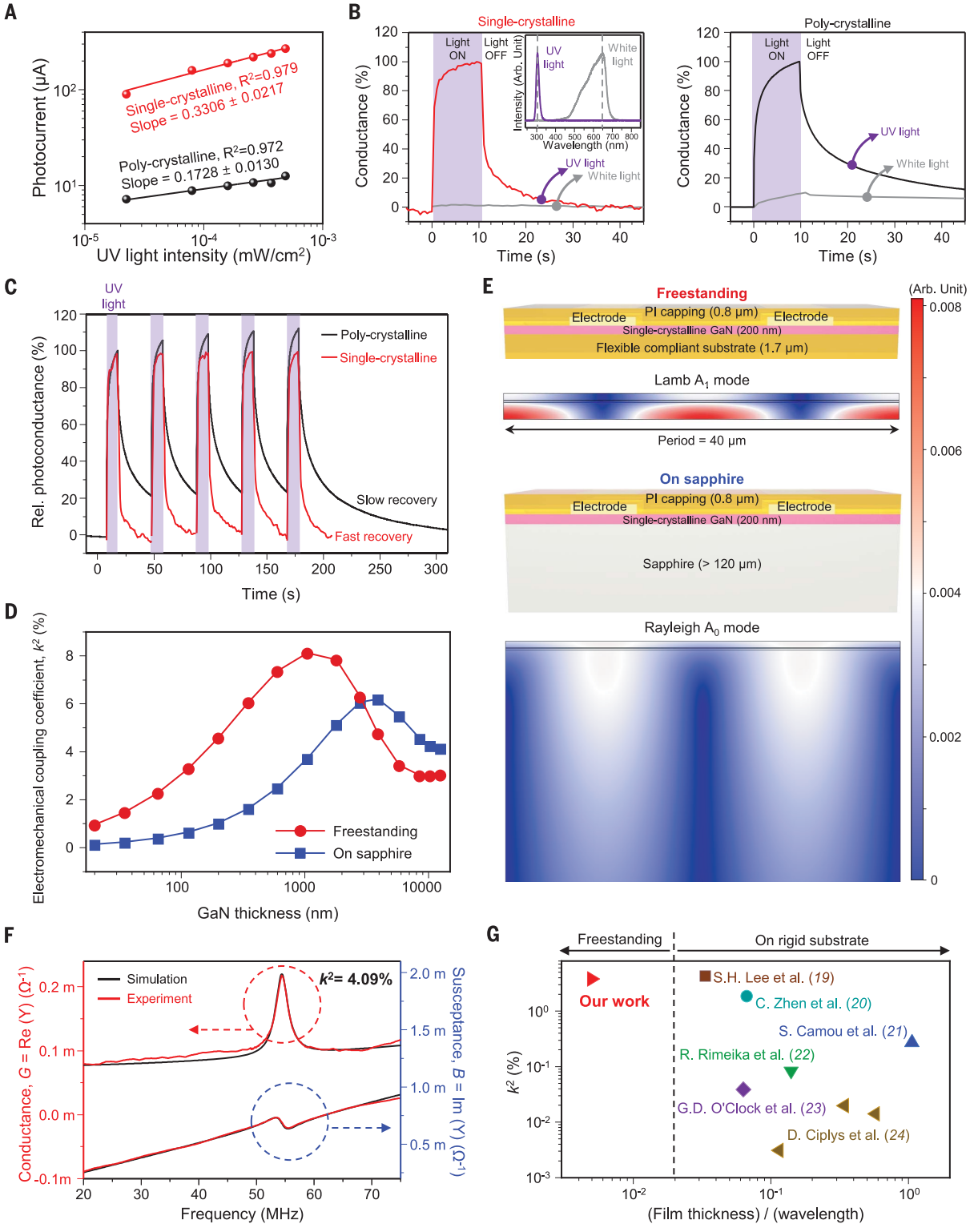

Fig. 2. High optoelectronic and surface acoustic performance of GaN-based single-crystalline e-skins. (**A** to **C**) GaN-metal Schottky diode UV sensors made of single-crystalline and polycrystalline GaN nanomembranes. (A) Responsivity of GaN UV sensors. The changes in photocurrent of GaN diodes in response to UV exposure with varying intensities. (B) Response and recovery speeds and selectivities for UV light over white light for (left) single-crystalline and (right) polycrystalline GaN UV sensors. The inset shows emission spectra of UV light and white light. (C) Consistency of UV response of GaN UV sensors. Slow switching speed of polycrystalline GaN sensors induces a gradual increase in remnant photoconductance. (**D** and **E**) Simulation result of SAW generation in freestanding GaN membrane and GaN on sapphire. (D) Calculated electromechanical coupling coefficient (k^2) of GaN SAW devices by the function of GaN thickness. (E) The displacement of GaN SAW. The freestanding GaN has higher displacement than GaN on sapphire. (**F**) Conductance and susceptance of our single-crystalline GaN SAW devices were used to extract experimental k^2. (**G**) Benchmark of extracted k^2 as a function of normalized thicknesses of GaN (*19*–*24*). Our freestanding single-crystalline GaN nanomembranes enable SAW generation at ultrathin GaN thickness, leading to k^2 as high as those of thick GaN layers on rigid substrates.

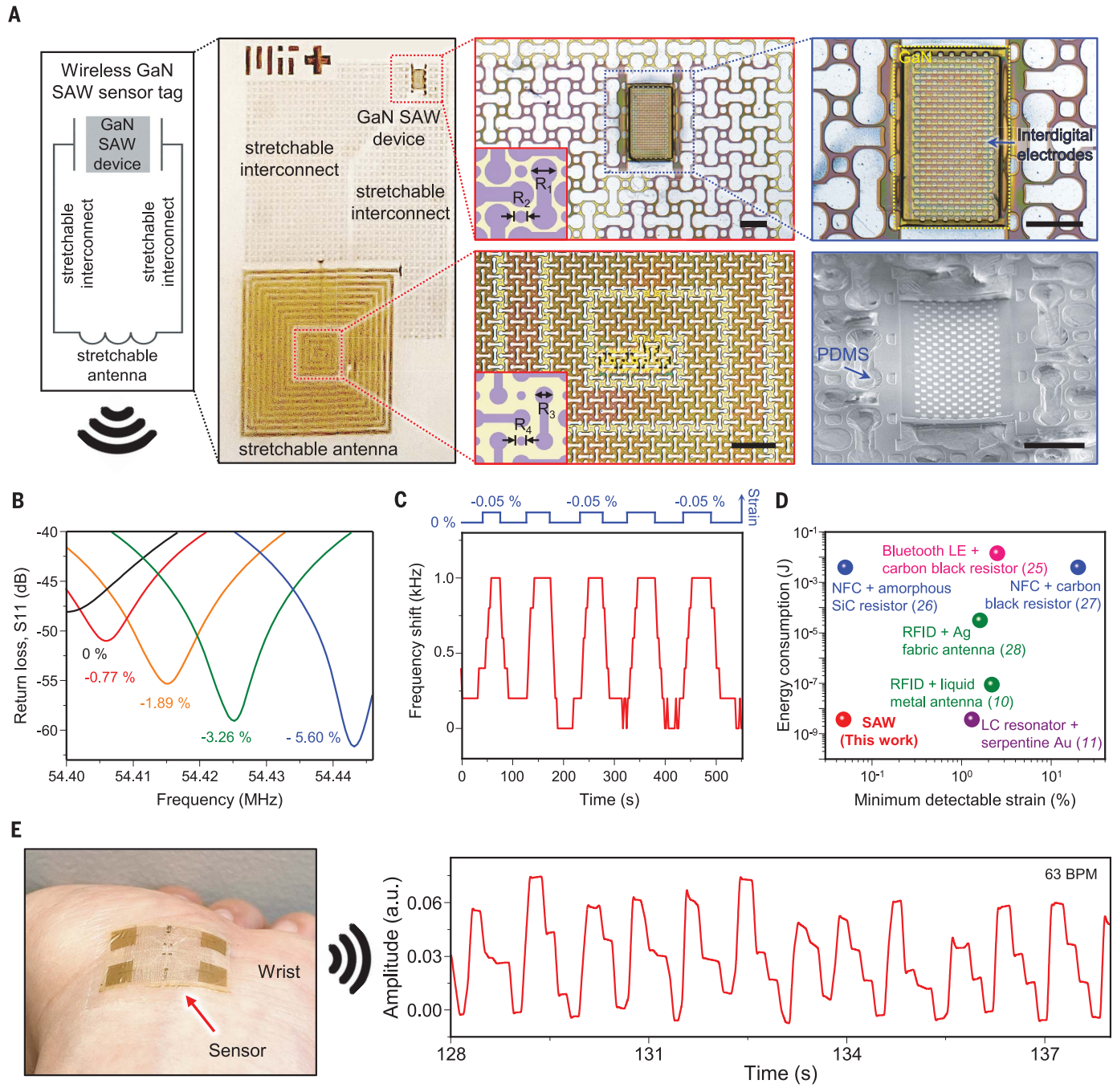

Fig. 3. Wireless GaN SAW strain sensors on e-skins free of communication chips or power source. (**A**) Schematic illustration and optical images of our wireless GaN SAW e-skin strain sensor. R1, R2, R3, and R4 in insets are 120, 50, 20, and 10 μm, respectively. Scale bars, 200 μm. (**B**) Resonant frequency shift as a function of strain for GaN SAW e-skin strain sensors. (**C**) Measurement of the minimum detectable strain of our GaN SAW e-skin strain sensors. (**D**) Benchmark of minimum detectable strain and energy consumption for battery-less wireless e-skin strain sensors reported previously (*10*, *11*, *25*–*28*). (**E**) Wireless pulse measurements using our GaN SAW e-skin strain sensors.

that responds sensitively to physiological activities, the changes of which can be detected wirelessly through the antenna. Although previous studies note that SAW generated by an ultrathin piezoelectric film grown on a sapphire substrate is relatively negligible owing to the strong binding of the film to the substrate (*17*, *18*), we have discovered that highly crystalline GaN films that are declamped from the substrate can generate SAWs with an ideal electromechanical coupling value.

Simulation of SAW generation in the GaN membrane (Fig. 2, D and E) showed that the electromechanical coupling coefficient k^2 is negligible for substrate-bound GaN films that are thinner than 300 nm (at a resonant frequency of ~54 MHz), because substrate binding alters the acoustic mode and substantially reduces the displacement amplitude of acoustic vibration. However, declamping of the GaN layer from the substrate substantially enhances electromechanical coupling by eliminating the binding effect. We experimentally confirmed that the k^2 value of our freestanding

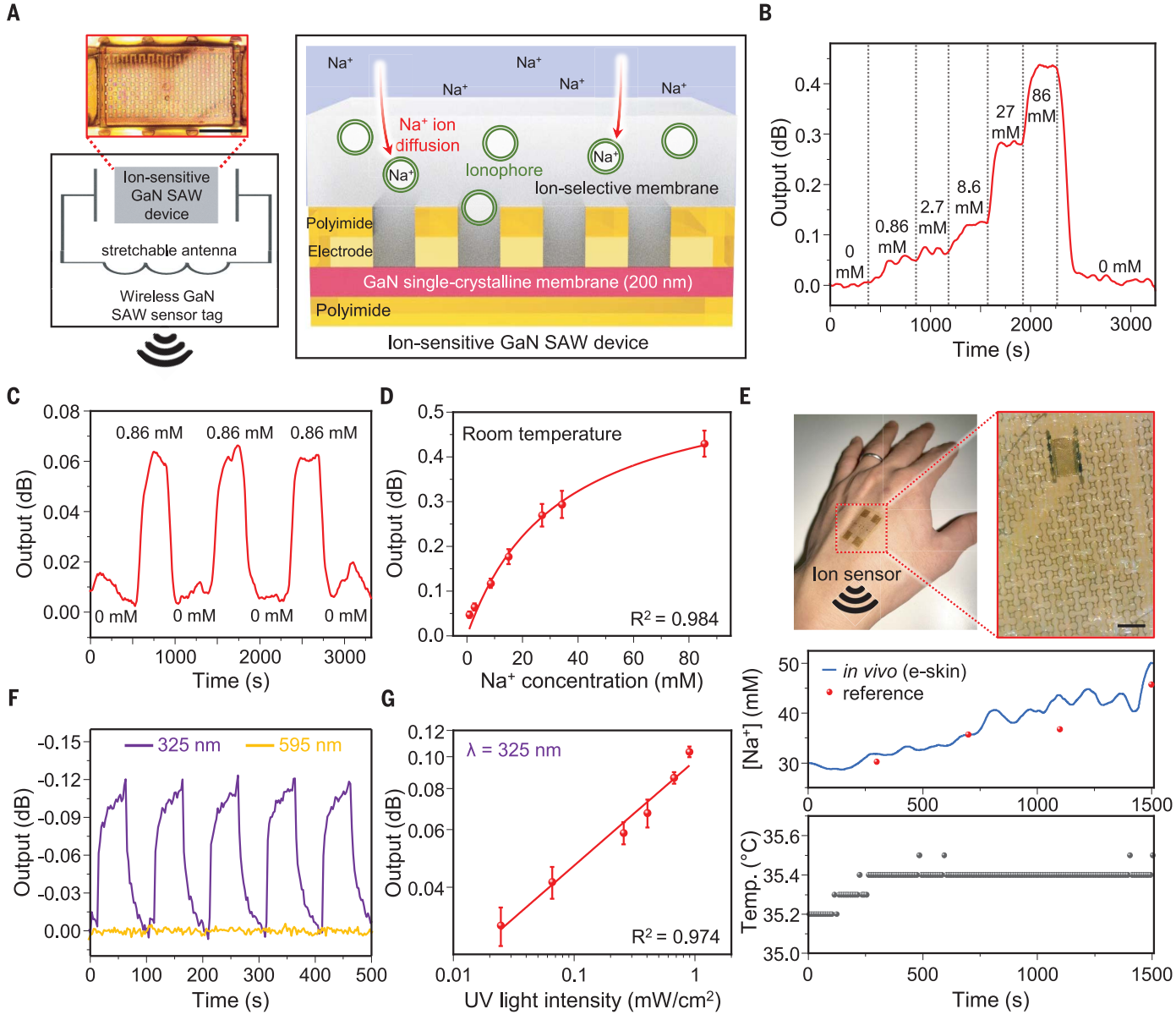

Fig. 4. Chip-free battery-less wireless GaN SAW ion sensors and UV sensors. (**A**) Schematic illustrations and optical microscope image of wireless ion sensors based on GaN SAW device coated with Na^+ ion–selective membranes. Scale bar, 200 μm. (**B**) Resonant frequency shift in the wireless signals obtained from a GaN SAW ion sensor in response to changes in Na^+ ion concentration. (**C**) Continuous wireless recordings collected from a SAW ion sensor during a series of alternating injections of 0.86 mM NaCl solution and distilled water over the e-skin, indicating consistent response and recovery characteristics. (**D**) Calibration of the responsivity of GaN SAW ion sensors to variation in Na^+ ion concentration. The error bars represent standard deviation in 5-min continuous measurements of the output signal for each concentration. (**E**) Photograph and microscopy image of an e-skin attached on the back of a hand (top), in vivo recordings of the variation in Na^+ ion concentration in sweat using wireless GaN SAW-based e-skin (blue) and a reference conductometer (red; middle), and in vivo recording of the skin temperature obtained by a commercially available thermometer (bottom). Putting a glove on the hand and placing heating pads on body induces sweating. Scale bar, 500 μm. (**F**) Continuous wireless recordings collected by a SAW UV sensor in response to exposures of UV light (purple) and white light (orange), indicating the sensor's selectivity. (**G**) Calibration of the responsivity of GaN SAW UV sensors to exposures of different UV light intensities. Each data point and error bar indicate the average and standard deviation, respectively, from eight different measurements.

200-nm-thick GaN obtained by 2DLT is close to the value of 4.09% (Fig. 2F) that was reported for a 2.0-μm-thick GaN SAW sensor on a sapphire substrate (*19*). As shown in the benchmark plot in Fig. 2G (*19*–*24*), the k^2 value of our GaN film is on par with values previously achieved by epitaxial GaN SAW sensors with greater thicknesses bound on sapphire wafers. A high k^2 value is essential for wireless detection, as it increases the signal-to-noise ratio in the resonant frequency shift of the SAW device on human skin.

Figure 3A shows the schematic illustration and microscopy images of our SAW-based chip-less wireless e-skin system. The GaN SAW device on a PDMS skin patch is designed to be freestanding and suspended in air to maximize device sensitivity (see supplementary text for detailed device structures). SAW resonant peak frequency changes in response to mechanical strain and mass due to absorption or desorption of ions, as well UV exposure due to optical absorption by GaN (see supplementary text for detailed mechanisms). By scanning

the return loss (S_{11}) over a range of frequencies using the external wireless reader, the resonant frequency of GaN SAW (53.95 MHz) was recorded wirelessly (see figs. S9 and S10 for details).

We demonstrated wireless strain sensing by first calibrating the resonant peak shifts in the SAW device in response to strain induced by bending the patch (Fig. 3B and fig. S11). Compared with previously reported battery-less wireless e-skin systems (*10*, *11*, *25*–*28*), our single-crystalline GaN–based e-skin exhibits higher strain sensitivity, smaller minimum detectable strain (0.048%), and lower power consumption owing to chip-less operation (Fig. 3, C and D, and figs. S12 and S13). Although LC resonator–based e-skins can also achieve low-power sensing (Fig. 3D), they suffer from low sensitivity and limited sensing modality outside that of mechanical stimuli (*11*, *29*, *30*). Their low sensitivity also necessitates highly sophisticated and costly vector network analyzers with low trace noise for wireless measurement.

The high strain sensitivity of a SAW sensor on e-skin allows the continuous chip-less wireless measurement of arterial pulse waves on the wrist. Figure 3E and movie S1 illustrate the continuously wireless monitoring of pulse signals using our e-skin. Figure S14 shows the results of daytime (worn for ~17 hours/day) monitoring of heart rate and pulse waveforms (measured after exercise) over 7 days, which demonstrates the reusability and long-term wearability of our e-skin. Continuous wireless recording of strain through bending (fig. S15) and stretching (10.3% strain; fig. S16) cycles shows that our e-skin can undergo reversible bending and stretching without fracturing of the GaN owing to thin, deformable metal interconnects (*30*).

Our SAW sensor's communication range is ~14 mm in the z direction, ~7.5 mm in the x direction, or a rotation of ~30° (fig. S17). The relatively short communication range leads to limited monitoring of heart rate during active body movement (fig. S18). Replacing the near-field electrically small antenna with a far-field loop antenna may lead to longer-distance wireless communication thanks to the very low power consumption of our SAW sensor (see Fig. 3D for power comparison; methods and fig. S13 for estimation of power consumption in SAW sensors; and supplementary text for wireless distance and comparison with chip-based e-skins).

We also explored the wireless monitoring of ion concentrations in sweat, which can serve as indicators for conditions such as hyponatremia, kidney failure, and hypertension (*31*), using our SAW-based e-skin platform. GaN has an extremely low dissolution rate in aqueous solutions and can therefore yield a stable, biocompatible sweat sensor. We coated the surface of a GaN SAW device with ion-selective membranes (ISMs) that can trap specific ions, which induces changes in the viscosity and mass of ISMs (see Fig. 4A, fig. S19, and table S2 for the design and composition of the SAW ion sensor). The resonant peak shifts in an ISM-coated SAW device can be used to wirelessly detect variation in ionic concentrations in surrounding fluids.

Figure 4, B to D, illustrates the results of in vitro wireless detection of Na^+ ions using an Na^+ ISM-coated GaN SAW device on e-skin. Continuous recordings in Fig. 4, B and C, indicate clear and consistent response and recovery of the output signal, collected by exposing the e-skin to aqueous NaCl solutions containing varying concentrations of Na^+ ions (see methods for detailed methodology). Calibration data in Fig. 4D, which represent the time-averaged response of the SAW sensor from 5-min continuous recordings, also indicate consistent sensor behavior. The detection limit of 0.86 mM represents a small value compared with the biologically relevant range of >10 mM in sweat, indicating the high sensitivity of the GaN SAW ion sensor. The sensor selectivity for Na^+ ions was confirmed by monitoring its response to flows of ionic solutions with different compositions (fig. S20).

Figure 4E shows images of a GaN SAW-based e-skin attached on the back of a hand for in vivo sweat analysis (see fig. S21 for measurement setup). Na^+ ion concentration in sweat was monitored simultaneously by a SAW sensor and a reference conductometer, while a commercial thermometer recorded skin temperature. The results show that the concentration of Na^+ ions in sweat gradually increases as perspiration continues (*5*). Integration of multiple types of ISMs on SAW devices may yield a wireless e-skin platform with improved versatility for sweat analysis.

Strong optoelectronic characteristics and piezoelectricity of GaN also enable wireless detection of UV light. SAW UV sensors (see fig. S22 for structures) respond to UV light (wavelength: ~325 nm) but not to white light (wavelength: ~595 nm), as shown in Fig. 4F. The results highlight the sensor's selectivity for UV owing to the matching bandgap of GaN, which eliminates the need for an optical filter and simplifies sensor design (fig. S23). Ion and UV (Fig. 4G) sensing capabilities of a GaN SAW-based e-skin illustrate the diverse sensing options that can be achieved using our chip-less wireless platform. Figure S24 also illustrates our sensors' capability to distinguish different types of input stimuli.

Here, we report a chip-free wireless e-skin platform based on SAW sensors made of free-standing ultrathin single-crystalline piezoelectric GaN films prepared by remote homoepitaxy and 2DLT to yield SAW devices with a high electromechanical coupling coefficient. SAW-based e-skins offer a versatile biomedical sensing platform with high sensitivity, low power consumption, and long-term wearability.

REFERENCES AND NOTES

1. Y. Lee *et al*., *Sci. Adv.* **7**, eabg9180 (2021).
2. D.-H. Kim *et al*., *Science* **320**, 507–511 (2008).
3. L. Tian *et al*., *Nat. Biomed. Eng.* **3**, 194–205 (2019).
4. H. U. Chung *et al*., *Science* **363**, eaau0780 (2019).
5. W. Gao *et al*., *Nature* **529**, 509–514 (2016).
6. D. Son *et al*., *Nat. Nanotechnol.* **9**, 397–404 (2014).
7. K. Myny, *Nat. Electron.* **1**, 30–39 (2018).
8. B. E. Jonsson, "An empirical approach to finding energy efficient ADC architectures," IMEKO TC4 International Workshop on ADC Modelling, Testing and Data Converter Analysis and Design 2011 (IWADC 2011) and IEEE 2011 ADC Forum, Orvieto, Italy, 30 June to 1 July 2011.
9. M. C. Vu *et al*., *ACS Appl. Mater. Interfaces* **12**, 26413–26423 (2020).
10. L. Teng *et al*., *Soft Robot.* **6**, 82–94 (2019).
11. X. Huang *et al*., *Adv. Funct. Mater.* **24**, 3846–3854 (2014).
12. Y. Kim *et al*., *Nature* **544**, 340–343 (2017).
13. H. Yeon *et al*., *Sci. Adv.* **7**, eabg8459 (2021).
14. Q. Hua *et al*., *Nat. Commun.* **9**, 244 (2018).
15. L. Shi, S. Nihtianov, *IEEE Sens. J.* **12**, 2453–2459 (2012).
16. R. Velazquez, A. Aldalbahi, M. Rivera, P. Feng, *AIP Adv.* **6**, 085117 (2016).
17. C. R. Gorla *et al*., *J. Appl. Phys.* **85**, 2595–2602 (1999).
18. A. Shankar *et al*., "Impact of gamma irradiation on GaN/sapphire surface acoustic wave resonators," 2014 IEEE International Ultrasonics Symposium, Chicago, IL, USA, 3 to 6 September 2014.
19. S.-H. Lee *et al*., *IEEE Trans. Electron Dev.* **48**, 524–529 (2001).
20. Z. Chen *et al*., *Chin. Phys. Lett.* **18**, 1418–1419 (2001).
21. S. Camou, T. Pastureaud, H. Schenk, S. Ballandras, V. Laude, *Electron. Lett.* **37**, 1053–1055 (2001).
22. R. Rimeika *et al*., *Phys. Status Solidi B* **234**, 897–900 (2002).
23. G. O'Clock Jr., M. Duffy, *Appl. Phys. Lett.* **23**, 55–56 (1973).
24. D. Čiplys *et al*., *Electron. Lett.* **36**, 591–592 (2000).
25. A. D. Mickle *et al*., *Nature* **565**, 361–365 (2019).
26. Y. Gao *et al*., *Adv. Funct. Mater.* **29**, 1806786 (2019).
27. R. Lin *et al*., *Nat. Commun.* **11**, 444 (2020).
28. O. O. Rakibet, C. V. Rumens, J. C. Batchelor, S. J. Holder, *IEEE Antennas Wirel. Propag. Lett.* **13**, 814–817 (2014).
29. S. Niu *et al*., *Nat. Electron.* **2**, 361–368 (2019).
30. D.-H. Kim *et al*., *Science* **333**, 838–843 (2011).
31. J. Choi, R. Ghaffari, L. B. Baker, J. A. Rogers, *Sci. Adv.* **4**, eaar3921 (2018).

ACKNOWLEDGMENTS

We thank M. R. Abdelhamid and A. P. Chandrakasan for allowing us to use their vector network analyzer. **Funding:** This work was supported by AMOREPACIFIC. **Author contributions:** Y.K. and Je.K. conceptualized this work. Y.K., J.M.S., H.Y., J.L., S.Ki., T.P., Y.S.L., and K.L. did the formal analysis. Y.K., J.M.S., J.S., Y.L., H.Y., K.Q., H.S.K., H.E.L., C.C., D.L., J.-H.K., J.A.P., Y.P., L.K., J.P., M.-C.P., H.K., S.-H.B., W.K., J.H., and Je.K. developed the methodology. Y.K., J.M.S., Y.L., J.S., H.Y., K.Q., H.S.K., C.K., H.E.L., C.C., H.K., B.-I.P., S.Ka., Ji.K., K.W., K.K., and W.K. performed experiments. Y.K., J.M.S., H.Y., and S.Ki. visualized data. H.Y. and Je.K. acquired funding. Je.K. supervised this project. Y.K., J.M.S., H.Y., H.E.L., and Je.K. wrote the original draft. All authors reviewed and edited the manuscript. **Competing interests:** Y.K., J.M.S., and Je.K. are inventors on patent application number 63/355531 submitted by the Massachusetts Institute of Technology that covers devices (e.g., resonators) comprising a single-crystalline material and related systems and methods. **Data and materials availability:** All data are available in the main text or the supplementary materials.

SUPPLEMENTARY MATERIALS

science.org/doi/10.1126/science.abn7325
Materials and Methods
Supplementary Text
Figs. S1 to S24
Tables S1 and S2
References (*32*–*42*)
Movie S1

Submitted 16 December 2021; accepted 7 July 2022
10.1126/science.abn7325

Science

Chip-less wireless electronic skins by remote epitaxial freestanding compound semiconductors

Yeongin KimJun Min SuhJiho ShinYunpeng LiuHanwool YeonKuan QiaoHyun S. KumChansoo KimHan Eol LeeChanyeol ChoiHyunseok KimDoyoon LeeJaeyong LeeJi-Hoon KangBo-In ParkSungsu KangJihoon KimSungkyu KimJoshua A. PerozekKejia WangYongmo ParkKumar KishenLingping KongTomás PalaciosJungwon ParkMin-Chul ParkHyung-jun KimYun Seog LeeKyusang LeeSang-Hoon BaeWei KongJiyeon HanJeehwan Kim

Science, 377 (6608), • DOI: 10.1126/science.abn7325

Chip-less electronic skin

Flexible electronic materials, or e-skins, can be limited by the need to include rigid components. A range of techniques have emerged to bypass this problem, including approaches for wireless communication and charging based on silicon, carbon nanotubes, or conducting polymers. Kim *et al*. show that epitaxially grown, single-crystalline gallium nitride films on flexible substrates can be used for chip-less, flexible e-skins. The main advantage is that the material is flexible and breathable, thus providing better comfort. The devices convert electrical energy into surface acoustic waves using a piezoelectric resonator. The resonator is sensitive to changes in strain, mass changes due to the absorption or loss of ions, and ultraviolet light, all of which can be used for different sensing measurements. —MSL

Science (ISSN) is published by the American Association for the Advancement of Science. 1200 New York Avenue NW, Washington, DC 20005. The title *Science* is a registered trademark of AAAS.